


Article

N-Carbamylglutamate Promotes Follicular Development by Modulating Cholesterol Metabolism in Yak Ovaries

Jia Zhou ^{1,†} , Jingjing Du ^{1,†}, Shuangming Yue ², Benchu Xue ¹, Lizhi Wang ¹, Quanhui Peng ¹ and Bai Xue ^{1,*}

¹ Animal Nutrition Institute, Sichuan Agricultural University, Chengdu 611130, China; zhoujia1@stu.sicau.edu.cn (J.Z.); 2020214037@stu.sicau.edu.cn (J.D.); xuebenchu@stu.sicau.edu.cn (B.X.); 12825@sicau.edu.cn (L.W.); 14101@sicau.edu.cn (Q.P.)

² Department of Bioengineering, Sichuan Water Conservancy Vocation College, Chengdu 611845, China; yueshuangming@stu.sicau.edu.cn

* Correspondence: xuebai@sicau.edu.cn

† These authors contributed equally to this work and should be considered co-first authors.

Abstract: This study aimed to investigate the effects of N-carbamylglutamate (NCG) supplementation on the follicular development of yaks to identify potential mechanisms essential for fertility in yaks. Twelve multiparous anoestrous female yaks were randomly assigned to two groups—Control (fed with a basal diet, $n = 6$) and NCG (basal diet supplemented with 6.0 g day⁻¹ NCG, $n = 6$). Yaks in the NCG group had higher numbers of large follicles (>5 mm in diameter) than those in the Control group. An RNA-sequencing analysis of yak ovaries revealed a total of 765 genes were differentially expressed between experimental groups, of which 181 genes were upregulated and 584 genes were downregulated following NCG supplementation. The results of a transcriptome functional analysis, qRT-PCR validation, and immunohistochemistry revealed that NCG supplementation increased angiogenesis and de novo synthesis of cholesterol in yak ovaries. NCG was also found to upregulate the gene expression of steroidogenic enzymes. Based on this, it was concluded that NCG supplementation promotes the follicular development of yaks mainly by affecting cholesterol metabolism to initiate steroidogenesis in ovaries. The results provide evidence for understanding the mechanisms responsible for NCG promoting follicular development of female yaks, which may contribute to the development and application of NCG in animal reproduction.



Citation: Zhou, J.; Du, J.; Yue, S.; Xue, B.; Wang, L.; Peng, Q.; Xue, B. N-Carbamylglutamate Promotes Follicular Development by Modulating Cholesterol Metabolism in Yak Ovaries. *Agriculture* **2021**, *11*, 825. <https://doi.org/10.3390/agriculture11090825>

Academic Editors: Domenico Vecchio, Marcello Rubessa and José Nélio de Sousa Sales

Received: 3 August 2021

Accepted: 26 August 2021

Published: 29 August 2021

Publisher's Note: MDPI stays neutral with regard to jurisdictional claims in published maps and institutional affiliations.



Copyright: © 2021 by the authors. Licensee MDPI, Basel, Switzerland. This article is an open access article distributed under the terms and conditions of the Creative Commons Attribution (CC BY) license (<https://creativecommons.org/licenses/by/4.0/>).

Keywords: yaks; N-carbamylglutamate; follicular development; cholesterol metabolism

1. Introduction

Yaks provide food (meat and dairy products), shelter (hair and hides), physical labour, and fuel (dung) for local herders living in high-altitude plateaus of China [1–3], making them an indispensable part of the pasture–livestock industry in these areas [4]. However, yak husbandry has been seriously restricted due to their low reproductive efficiencies caused by their seasonal breeding characteristics, restricted oestrus cycles, and conception that only occurs in the warm season (July–October) [3,5]. In addition, a large proportion of yak cows experience long postpartum anoestrus periods and begin their next oestrus cycles only two–three years after calving, rather than in the breeding season of the next year [3,6]. Thus, most yaks calve once every two years or twice in three years [5], with an average annual reproduction rate of 40–60% [3]. For domestic beef cows, complete uterine involution following a trouble-free calving only takes ~30 days; females are then ready for the next ovarian cycle [7]. The duration of postpartum anoestrus is mainly determined by the time required for the recruitment of new follicles and the establishment of follicle dominance [8]. Therefore, a straightforward strategy to shorten postpartum anoestrus periods and improve fertility in yaks might be to accelerate the resumption of postpartum follicular activity.

Ovarian follicles contain an oocyte surrounded by granulosa cells, which are in turn enclosed by layers of thecal cells [9]. Ovarian folliculogenesis is a complex physiological process controlled by a variety of endocrine, paracrine, and autocrine factors. In this process, several steroid hormones affect cell proliferation, apoptosis, and angiogenesis within the follicle to regulate follicular development [10]. The steroid hormones oestrogen and progesterone are mainly synthesized by cholesterol in follicular cells and the corpus lutea, respectively. Although cholesterol biosynthesis occurs in almost all tissues [11], the amounts of cholesterol synthesised in the ovarian tissues are inadequate for the amounts required in steroidogenesis [12]. Therefore, the ovaries require a steady supply of cholesterol from low-density lipoproteins (LDLs) and high-density lipoproteins (HDLs) in blood.

Since the ovaries are dependent on the blood vessels for nutrients (including cholesterol), oxygen, hormones, and cytokines to support follicular progression [13], ovarian follicular development is intimately associated with ovarian angiogenesis. The expression of vascular endothelial growth factor A (VEGFA) is used as a biomarker to gauge ovarian function and status [14]. Stimulation with VEGFA has been shown to promote maturation of primary follicles into secondary follicles in cows [15]. Other studies have also demonstrated that injection of vascular endothelial growth factor (VEGF) gene fragments into ovaries could stimulate follicular development in female rats [16,17], mice [18], and pigs [19], whereas, the inhibition of VEGFA stimulation had a negative effect on ovarian follicular growth and development in female rats [20] and mice [21]. In addition, compared to atretic follicles, healthy antral follicles had higher levels of VEGFA expression [22] and better vascular development [23].

N-carbamoyl glutamic acid (NCG), a structural analogue of N-acetylglutamate, is low in rumen degradation [24] and available from chemical synthesis with low costs [25], which is potentially a relatively cheap source of feed additive. NCG is known to enhance the synthesis of endogenous arginine by activating carbamoyl phosphate synthase-1 and pyrroline-5 carboxylate synthase [25]. Subsequently, this arginine is converted to nitric oxide (NO) by nitric oxide synthase (NOS), which in turn mediates VEGFA-induced proangiogenic functions. NCG has been shown to increase plasma levels of NO in pigs [26] and lambs [27], upregulate gene expression of VEGFA in pigs [28], and increase epithelial NOS (eNOS) levels in lambs [27]. NCG supplementation has also been shown to promote follicular development by promoting ovarian angiogenesis in chickens [13]. Therefore, it is highly likely that NCG, by promoting ovarian angiogenesis, improves the supply of cholesterol to the ovaries and contributes to ovarian follicular development. NCG is also known to be involved in the regulation of cholesterol biosynthesis. Dietary supplementation with NCG suppressed the AMP-activated protein kinase (AMPK) signalling pathway in the intestinal mucosa of suckling lambs [29]. The inhibition of AMPK promotes the nuclear transfer of the sterol regulatory element binding protein 2 (SREBP2; which is a master transcription factor for enzymes involved in cholesterol biosynthesis) and the expression of 3-hydroxy-3-methylglutaryl-coenzyme A reductase (HMGCR; the enzyme that catalyses the rate-limiting in cholesterol biosynthesis) [30]. Due to its positive effects on angiogenesis and cholesterol biosynthesis, we hypothesized that NCG supplementation could enhance ovarian follicular development in yaks. To test this hypothesis, RNA-Seq was used to analyse the transcript profiles of two groups of yaks—a control group (not supplemented with NCG) and a group that received feed supplemented with NCG. In this study, we investigate the effects of NCG on ovarian follicular development in yaks, as well as the role of ovarian cholesterol metabolism in this process.

2. Materials and Methods

All experimental protocols used in this study were performed in accordance with the rules in the 'Guide for the Care and Use of Laboratory Animals' constituted by the Institutional Animal Care and Research Committee of Sichuan Agricultural University.

2.1. Animals and Experimental Design

The experiment was conducted at the Dujiangyan Oujiapo Cattle Farm (Chengdu, China; latitude 30.59° and longitude 103.37°) from August to October 2020. Fourteen multiparous non-pregnant female yaks (parities = 1.21 ± 0.43 ; body weight (BW) = 167.8 ± 20.81 kg; age = 4.43 ± 0.85 years; mean \pm SD) were selected and divided into 7 blocks based on BW, parity, and age, and randomly allocated into two groups—the Control group (fed with basal ration) and NCG group (fed with basal ration + NCG (6 g/day per yak, 97% purity; from the National Feed Engineering Technology Research Center, Beijing, China)). After two weeks of adaptation, all yaks were fed daily with a total mixed ration diet in two meals (one at 0700 h and the other at 1700 h). The diet was formulated according to the Chinese Beef Cattle Raising Standard 2004 (NY/T 815–2004) to meet 100% of the estimated nutrient requirements for maintaining yaks. The ingredients and nutrient composition of the diet are provided in Supplementary Table S1. Diets were offered to individual yaks in tie-stalls, and the supplementary NCG was added by top-dress feeding onto the total mixed ration. The dose of NCG (6 g/day per yak) fed was based on previous studies in ewes [31], dairy cows [32], pigs [26], and chickens [13]. Water was ad libitum to the yaks ad libitum throughout the experimental period.

The protocol for oestrus synchronization was carried out as described previously [33–35] with minor modifications. In brief, all yaks were pre-synchronized by intravaginal device of a pessary (containing 1.38 g of progesterone; Ningbo Sansheng Biological Technology Co., Ltd., Ningbo, China) at the beginning of the experiment (day 0). On day 12, pessaries were removed and the yaks were given intramuscular injections of a prostaglandin $F_{2\alpha}$ analogue (PG, Estrumate, equivalent to 0.4 mg cloprostenol; Ningbo Sansheng Biological Technology Co., Ltd. Ningbo, China) to induce luteolysis, oestrus, and ovulation of the first-wave dominant follicle. Onset of oestrus was detected using a castrated yak bull (between days 14 and 16). One yak which did not exhibit oestrus during the monitoring period in the Control group, and one yak with abnormal feed intake in the NCG group were removed from this study. Finally, a total of twelve yaks in both groups (Control group, $n = 6$ and NCG group, $n = 6$) were slaughtered on day 32, equivalent to the luteal phase of the next oestrous cycle, and at the predicted time of selection of the third-wave dominant follicle [36].

2.2. Sample Collection

Blood samples (5 mL) were collected in plain evacuated serum tubes from the yaks' jugular veins on days 28, 30, and 32 before the morning feeding. Blood samples were centrifuged at 3000 rpm for 10 min at 4 °C to obtain serum, which was stored at -20 °C for further analysis. The ovaries collected from each yak were weighed and placed in culture dishes with cold Dulbecco's phosphate-buffered saline (D-PBS; Gibco, Grand Island, NY, USA). A total of 24 ovaries from 12 yaks were collected. Each ovary exhibited an obvious corpus luteum, confirming that all yaks were in the luteal phase of the oestrous cycle as expected. All visible follicles (diameter > 1 mm) in the left-side ovary of each yak were carefully dissected from the stroma with surgical scissors and dissecting forceps. Then, a graph paper grid (accuracy = 1 mm) was placed under the dish to count the numbers of follicles of different diameters. We classified the follicles into four grades based on diameter (as is customary for yaks) [37]—1–5 mm, >5 mm, 5–10 mm, and >10 mm—and calculated the average number of follicles in each category. The average number of follicles in each category between the two groups was statistical analysed. The remainder of the left-side ovary was rapidly frozen in liquid nitrogen and transferred to a -80 °C refrigerator until it was used for RNA extraction. The right-side ovary was fixed in 4% paraformaldehyde for morphological and biochemical analysis.

2.3. Serum Biochemistry and Hormone Assays

The serum concentrations of total cholesterol (TC), high-density lipoprotein cholesterol (HDL-C), low-density lipoprotein cholesterol (LDL-C), non-esterified fatty acids (NEFA),

and triglycerides (TG) were determined using appropriate kits (Beijing Strong Biotechnologies, Beijing, China) and a Hitachi 3100 automatic biochemical analyser (Hitachi High Technologies Co., Ltd., Tokyo, Japan). Serum oestradiol, progesterone, follicle stimulating hormone (FSH), and luteinizing hormone (LH) levels were measured with commercial ELISA kits (MEIMIAN, Yancheng, China) according to the manufacturer's instructions.

2.4. Ovary Histology

Ovaries were fixed in 4% paraformaldehyde, dehydrated with graded ethanol, and embedded in paraffin. Subsequently, paraffin-embedded ovaries were sectioned into 5 µm thick sections for immunohistochemistry (IHC) and immunofluorescence (IF) procedures. The IHC and IF procedures were performed as previously described [13,38]. Briefly, sections were placed in 3% hydrogen peroxide and incubated at room temperature in darkness for 25 min to remove endogenous peroxidase activity and then blocked with 3% bovine serum albumin. Following this, the sections were incubated overnight at 4 °C with rabbit anti-VEGF (1:600, Wuhan Servicebio Technology Co., Ltd., Wuhan, China) and rabbit anti-CD31 (1:50, Abcam, Cambridge, MA, USA) antibodies. Next day, the sections were washed and incubated at room temperature for 50 min with anti-goat HRP-labelled secondary antibody (Sigma-Aldrich, St. Louis, MO, USA). Finally, the sections for IF staining were incubated with 4',6-diamidino-2-phenylindole (DAPI) solution at room temperature for 10 min in a dark place; the sections for IHC staining were incubated with freshly prepared 3,3'-diaminobenzidine tetrahydrochloride (DAB) colour developing solution at room temperature for 15 min in a dark place. Images were obtained using a Nikon Eclipse Ci-L microscope (Nikon Instruments, Tokyo, Japan) and quantification of IHC staining was performed using Image-Pro Plus 6.0 (Media Cybernetics, Maryland, MD, USA) as described previously [39].

2.5. RNA Extraction, cDNA Library Construction, and Sequencing

Total RNA was extracted from the ovarian tissue using the Trizol reagent kit (Invitrogen, Carlsbad, CA, USA) as per the manufacturer's instructions. The purities and concentrations of total RNA extracts were evaluated with a NanoDrop 2000 spectrophotometer (Thermo Fisher Scientific, Inc., Waltham, MA, USA). In addition, an Agilent 2100 Bioanalyzer (Agilent Technologies, Palo Alto, CA, USA) and RNase-free agarose gel electrophoresis assays were also used to assess and check RNA quality. Only samples with RNA integrity numbers >7.0 were used in further procedures. Oligo(dT)-enriched mRNA was treated with fragmentation buffer, and cDNA of the RNA fragments were obtained through reverse transcription using random primers. The cDNA fragments were purified using the QiaQuick PCR Extraction Kit (QIAGEN, Venlo, The Netherlands), end repaired, and had poly(A) tails added to them before they were ligated to Illumina sequencing adapters. The TruSeq Stranded mRNA LTSample Prep kit (Illumina, San Diego, CA, USA) was used to construct the cDNA library as per the manufacturer's instructions. A total of 6 RNA-Seq libraries (3 for the Control group and 3 for the NCG group) from yak ovarian tissues were constructed on an Illumina HiSeq2500 platform (Gene Denovo Biotechnology Co., Ltd., Guangzhou, China). The raw sequence data obtained were deposited at NIH's Sequence Read Archive (SRA) under the accession numbers SRR14847984, SRR14847985, SRR14847986, SRR14847987, SRR14847988, and SRR14847989 (<https://dataview.ncbi.nlm.nih.gov/object/PRJNA738716>, [accessed on 8 August 2021]).

2.6. Quality Control and Mapping

To obtain high quality and clean reads, the raw reads containing adapters, undetermined bases, or low-quality bases were further filtered using the FastQC version 0.11.8 (<http://www.bioinformatics.babraham.ac.uk/projects/fastqc>, [accessed on 1 March 2021]) [40] and checked with Trimmomatic version 0.36 (<http://www.usadellab.org/cms/index.php?page=trimmomatic>, [accessed on 2 March 2021]). Low-quality reads and those containing poly-N sequences were removed [41]. The Phred scores of the clean reads from

downstream reprocessing and analysis exceeded 30 and were equivalent to the benchmark accuracy of >99.9%. The paired-end clean reads were mapped to the yak genome (*Bos mutus*) with Hisat2 version 2.1.0 (<http://www.ccb.jhu.edu/software/hisat/index.shtml>, [accessed on 2 March 2021]) [42].

2.7. RNA-Seq Data Analysis

The mapped reads of each sample were assembled with StringTie version 1.3.1 (<http://ccb.jhu.edu/software/stringtie/gff.shtml>, [accessed on 4 March 2021]) [43,44] through a reference-based approach. For each transcription region, StringTie software was used to calculate an FPKM (fragments per kb per million reads) value to quantify its expression levels and variation. Differentially expressed genes (DEGs) in ovaries from Control and NCG groups were identified using the DESeq2 software (<http://www.bioconductor.org/packages/release/bioc/html/DESeq2.html>, [accessed on 4 March 2021]) [45]. The genes with corrected *p*-values < 0.05 and absolute fold change (FC) values ≥ 1.5 were considered to be DEGs. All DEGs were mapped to gene ontology (GO) terms in the Gene Ontology database (<http://www.geneontology.org/>, [accessed on 5 March 2021]) and annotated by GO functional enrichment to identify their main biological functions. Gene ontology and pathway terms with corrected *p*-values < 0.05 were selected for further analyses.

2.8. RT-PCR Analysis

Candidate DEGs were selected for functional validation using RT-PCR analysis. Satisfactory RNA extracts from ovaries were reverse transcribed into cDNA with PrimeScript™ RT reagent Kit (Takara, Kyoto, Japan). Quantitative Real-Time PCR (qRT-PCR) was carried out with a SYBR Premix Ex Taq™ (Vazyme Biotech Co., Ltd., Nanjing, China) on the QuantStudio™ 6 Real-Time PCR System (Thermo Fisher Scientific, Waltham, MA, USA) as per the manufacturer's instructions. Relative gene expression levels of the NCG group were expressed as fold changes relative to the average mRNA abundances of the genes in the Control group; these were analysed using the comparative cycle threshold ($2^{-\Delta\Delta C_t}$) method [46] with β -actin and glyceraldehyde-3-phosphate dehydrogenase gene (GAPDH) as internal reference genes. The primer sequences used in these procedures are listed in Supplementary Table S2.

2.9. Statistical Analysis

Data for the numbers of follicles and weights of ovaries, serum biochemistry and hormones, percentage of area positive for VEGF, and relative expression of genes were analysed using the independent two-sample *t*-test using the SPSS 17.0 software (SPSS Inc., Chicago, IL, USA) and reported as mean \pm SEM. Volcano plot, column of the DEGs and GO enrichment analysis was carried out with OmicShare tools, which is a free online platform for data analysis (www.omicshare.com/tools, [accessed on 12 April 2021]). Each individual yak was regarded as an independent experimental unit. Following the $2^{-\Delta\Delta C_t}$ method, the mean value of ovarian gene expression of yaks in the Control group was set to 1.00. Statistical significance was set at $p < 0.05$.

3. Results

3.1. Follicular Development

The numbers of follicles and weights of ovaries in the Control and NCG groups are presented in Table 1. NCG did not seem to affect the numbers of follicles in the >10 mm size class or the weights of the ovaries. As compared to the Control group, the mean numbers of follicles in the NCG group were significantly lower ($p = 0.051$). However, the NCG group ovaries had significantly larger numbers of follicles in the 5–10 mm and >5 mm size classes ($p < 0.05$).

Table 1. The mean numbers of follicles in different size classes and weights of ovaries between the two groups.

Items	Control	NCG	<i>p</i> -Value
No. of visible follicles (diameter, <i>n</i>)			
1–5 mm	17.00 ± 4.41	6.67 ± 1.50	0.051
5–10 mm	1.33 ± 0.42	3.00 ± 0.45	0.022
>5 mm	1.50 ± 0.50	3.33 ± 0.42	0.019
>10 mm	0.17 ± 0.17	0.33 ± 0.21	0.549
Ovarian weight (g)			
Left-side ovaries	1.59 ± 0.27	1.30 ± 0.13	0.347
Right-side ovaries	1.52 ± 0.20	1.35 ± 0.24	0.582
Total weight	3.11 ± 0.46	2.65 ± 0.35	0.435

Control: yaks fed with basal ration; NCG: yaks fed with basal ration + NCG (6 g/day per yak); No: number. Data are represented as mean ± SEM, *n* = 6. *p* < 0.05 was considered statistically significant.

3.2. Serum Biochemistry and Hormones

Effects of NCG on the concentrations of different serum components, including hormones, are shown in Figure 1. The serum concentrations of oestradiol were significantly higher on days 28 and 32 (*p* < 0.05 and *p* < 0.01, respectively) in the NCG group as compared to those in the Control group. In addition, yaks in the NCG group also had significantly higher levels of serum FSH on day 32 (*p* < 0.05) as compared to those in the Control group. Yaks in the NCG group did not have significantly different levels of serum TC, LDL-C, HDL-C, NEFA, or TG as compared to those in the Control group.

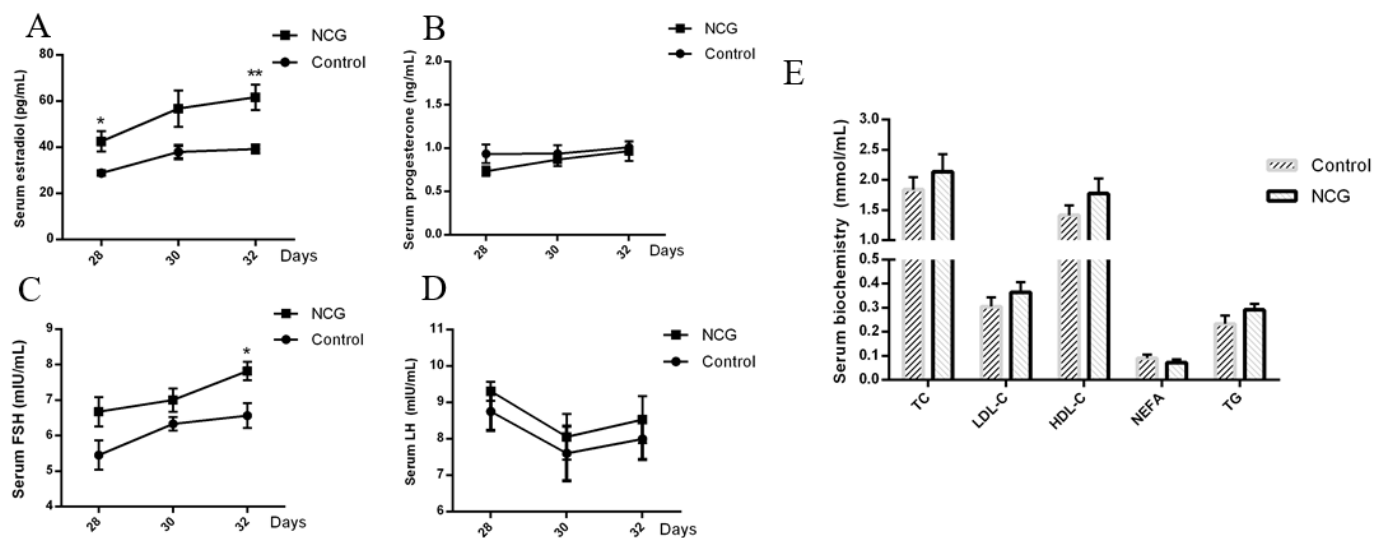


Figure 1. Effects of NCG N-carbamylglutamate on serum components, including hormones. Serum levels of (A) oestradiol, (B) progesterone, (C) follicle stimulating hormone (FSH), and (D) luteinizing hormone (LH) on days 28, 30, and 32. (E) Serum levels of total cholesterol (TC), high-density lipoprotein cholesterol (HDL-C), low-density lipoprotein cholesterol (LDL-C), non-esterified fatty acid (NEFA), and triglyceride (TG) on day 32. Data are represented as mean ± SEM, *n* = 6. * *p* < 0.05, ** *p* < 0.01.

3.3. Transcriptome and Functional Analyses of Ovarian Tissues

A transcriptome analysis of the ovarian tissues from Control and NCG groups led to the identification of 765 DEGs (FDR ≤ 0.05) (Figure 2A). Relative to the Control group, 584 genes were downregulated and 181 genes were upregulated in the NCG group (Figure 2B). Functional classifications (including biological processes, molecular functions, and cellular components) of these DEGs identified 1053 enriched GO terms (*p* < 0.05). The top twenty enriched GO terms are presented in Supplementary Figure S1 and the top ten terms in each functional classification are presented in Figure 3. Within the GO

domain for biological processes (Supplementary Figure S2A), most DEGs were assigned to a positive regulation of biological processes (GO: 0048518; 212 genes), developmental processes (GO: 0032502; 211 genes), and anatomical structure development (GO: 0048856; 200 genes). Within the GO domain for molecular functions (Supplementary Figure S2B), most DEGs were assigned to binding (GO: 0005488; 499 genes), protein binding (GO: 0005515; 335 genes), and ion binding (GO: 0044464; 188 genes) functions. Within the GO domain for cellular components (Supplementary Figure S2C), most DEGs were assigned to cell parts (GO: 00043167; 444 genes), cell (GO: 0005623; 444 genes), and cytosol (GO: 0005829; 117 genes).

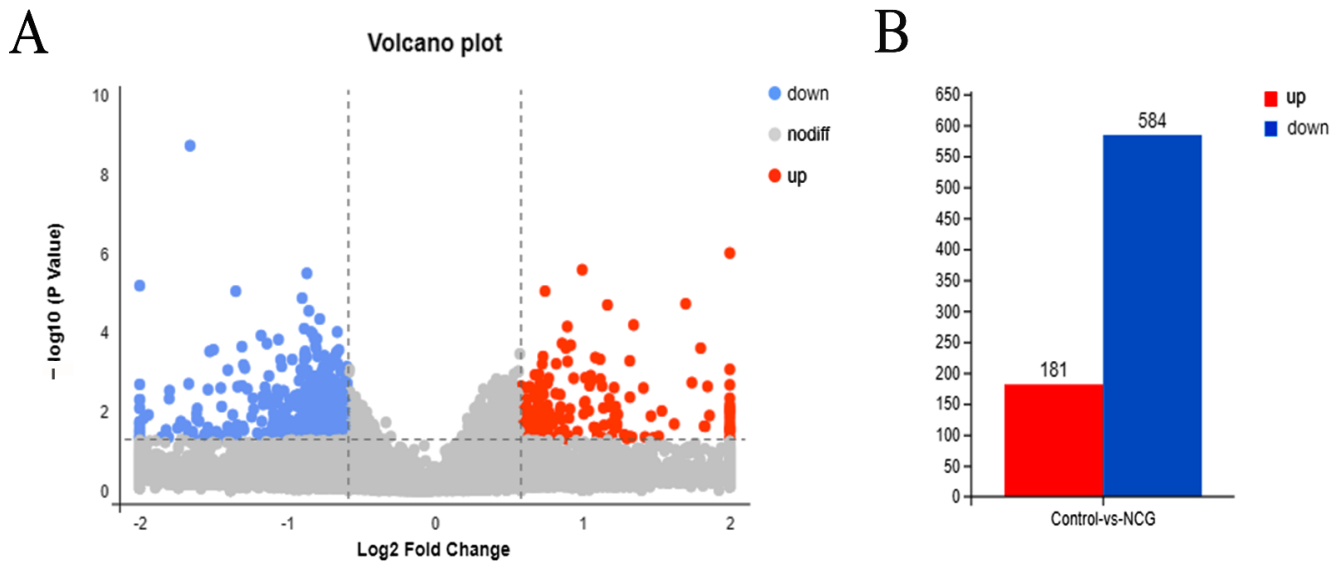


Figure 2. Volcano plot (A) and column (B) of the differentially expressed genes (DEGs) in ovarian tissues of Control and NCG group yaks. Blue, red, and grey dots denote downregulated ($FDR \leq 0.05$), upregulated ($FDR \leq 0.05$), and non-differentially expressed ($FDR > 0.05$) genes in ovarian tissue from yaks in the NCG group ($n = 3$) as compared to those in the Control group ($n = 3$).

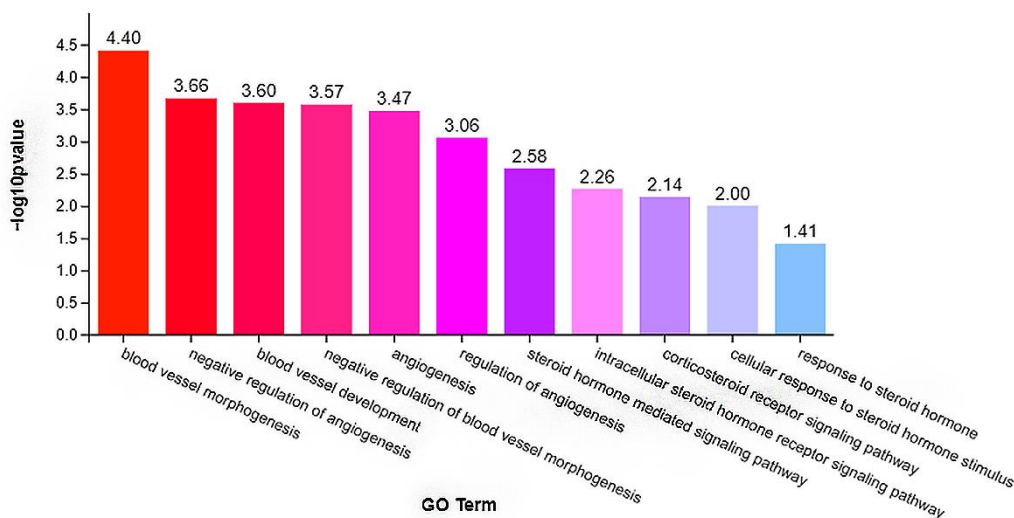


Figure 3. Gene ontology (GO) terms related to steroid hormone synthesis and angiogenesis.

To further investigate the metabolic pathways through which NCG could be regulating follicular development, we screened the results of the GO analysis for enriched clusters related to steroid hormone synthesis and angiogenesis (Figure 3). We also investigated the expression profiles of the top-ranked genes in these clusters and additional genes involved in cholesterol biosynthesis, and conducted hierarchical Euclidean distance

analyses (Figure 4). In the NCG group, a large proportion of genes related to cholesterol and steroid hormone synthesis, as well as angiogenesis, were upregulated, indicating that NCG affected these processes in yak ovaries and was likely to have affected follicular development.

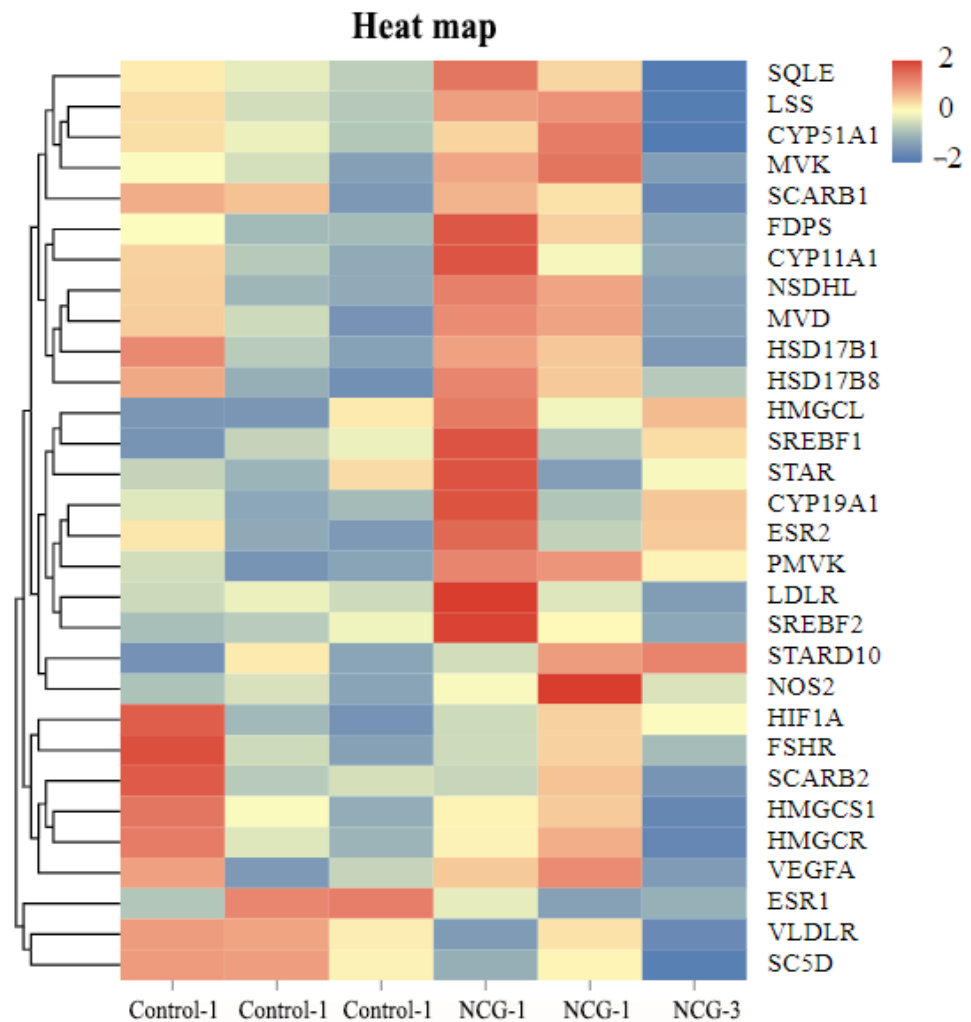


Figure 4. The expression profiles of genes related to steroid hormone metabolism, cholesterol synthesis, and angiogenesis as measured by RNA-Seq and represented in a heat map. The differences in gene expression levels are expressed in different colours, as illustrated in the legend.

3.4. Ovarian Angiogenesis

To verify the effects of NCG on ovarian angiogenesis, we examined the expression of genes related to angiogenesis in the ovarian tissues of Control and NCG groups using RT-PCR. Vascular development within the ovaries was also investigated using IHC and IF staining. Compared to the Control group, the expression of the *VEGFA* gene was upregulated in the NCG group, though this was not statistically significant ($p = 0.097$); however, expression levels of the *NOS2* gene were significantly higher in the NCG group ($p = 0.015$) as compared to those in the Control group (Figure 5D). Vascular development in the ovarian tissues of yaks was significantly higher in the NCG group than in those of the Control group as indicated by the higher levels of VEGF and CD31 detected using IHC and IF staining (Figure 5A,C).

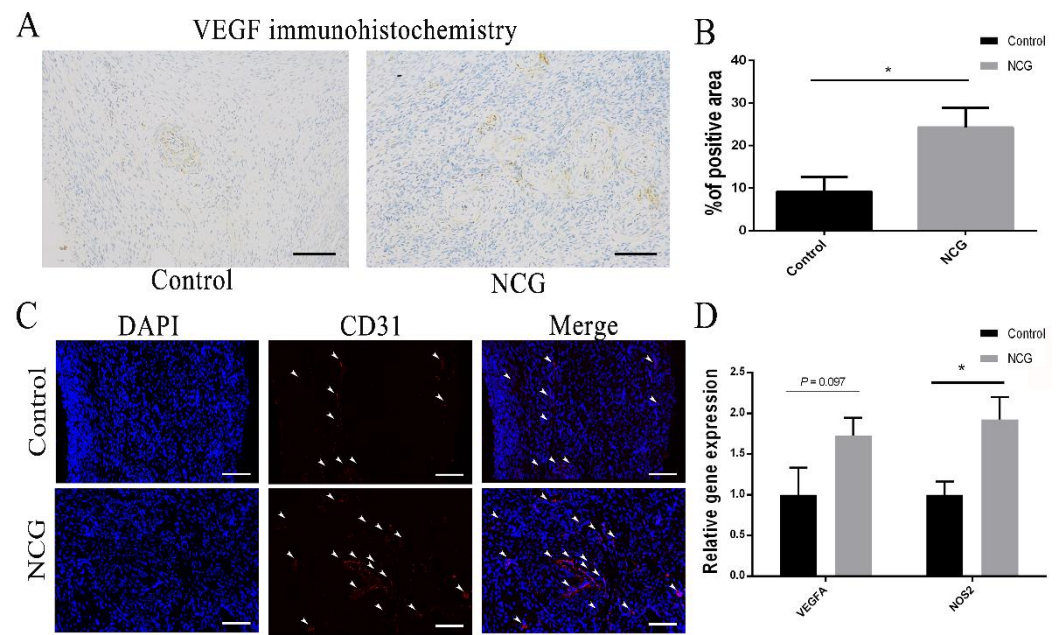


Figure 5. Effects of NCG on angiogenesis in yak ovaries. (A) Immunohistochemistry (IHC) to detect vascular endothelial growth factor (VEGF) in the ovaries. Scale bar: 50 μ m. (B) Percentage of area positive for VEGF in the ovaries was calculated using Image-Pro Plus software. (C) Immunofluorescence (IF) staining to detect CD31. White arrowheads indicate blood vessels. Scale bar: 50 μ m. (D) Relative gene expression levels of VEGFA and NOS2. Data are represented as mean \pm SEM, $n = 6$. * $p < 0.05$.

3.5. Expression of Genes Related to Cholesterol Metabolism

The gene expression profiles of scavenger receptor class B member 1 (*SCARB1*), scavenger receptor class B member 2 (*SCARB2*), sterol regulatory element binding transcription factor 2 (*SREBP2*), and lanosterol synthase (*LSS*) ($p < 0.01$), as well as oestrogen receptor 2 (*ESR2*) and squalene monooxygenase (*SQL*) ($p < 0.05$), were significantly higher in the NCG group as compared to those in the Control group (Figure 6). Additionally, the gene expression steroidogenic acute regulatory protein (*STAR*, $p = 0.072$) and hydroxysteroid 17-beta dehydrogenase 1 (*HSD17B1*, $p = 0.089$) showed an increasing trend in the NCG group.

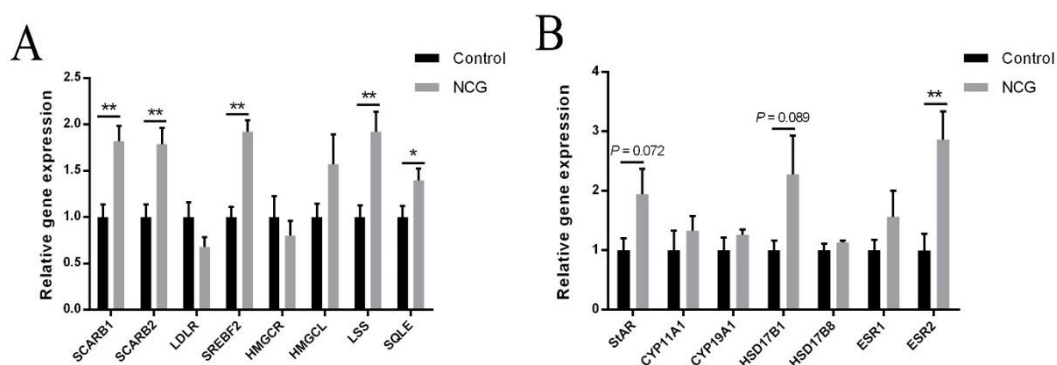


Figure 6. Effects of NCG on the relative expression profiles of genes related to cholesterol metabolism in yak ovaries. (A) Genes related to cholesterol biosynthesis. (B) Genes related to steroid hormone biosynthesis. Data are represented as mean \pm SEM, $n = 6$. * $p < 0.05$, ** $p < 0.05$.

4. Discussion

In cattle, the synchronous growth of dozens of small ovarian follicles occurs two or three times during a single oestrous cycle [36]. The growth periods of these follicles are known as 'follicular waves' [47]. In most cases, only one dominant (the largest) follicle continues to grow in the last (third) follicular wave (which occurs on days 15–16 of the oestrous cycle) and becomes the mature ovulatory follicle (12–20 mm in diameter), while the remaining follicles in the original cohort undergo atresia [48,49]. Based on this progression, ovarian tissues were collected from experimental animals (yaks) on the 16th day of the oestrous cycle in this study.

The size of the follicle that an oocyte originates from is frequently used to study and evaluate the development of oocytes [50] as there is a direct correlation between oocyte development and follicle size in cattle. Most mammalian oocytes are lost in the physiological process of atresia, and only those oocytes from dominant follicles proceed to ovulation [51]. The development of bovine oocytes in follicles <3 mm in size was halted before the 16-cell stage, while oocytes in larger follicles continued to grow [52]. Therefore, we consider follicle size to be a convenient marker for oocyte development.

In the NCG group, the numbers of follicles in the 1–5 mm size class were lower, while those in the 5–10 mm class were higher as compared to those in the Control group. Since whole follicles disappear during follicular atresia, we suggest that NCG supplementation either accelerated the development of follicles in the 1–5 mm size class, or delayed atresia in follicles >5 mm; it is also possible that more follicles in the >5 mm class in the Control group underwent atresia without NCG supplementation. Numerous studies have reported that concentrations of oestradiol and the ratios of oestrogen to progesterone in healthy follicles are much higher than those in follicles fated to undergo atresia [53,54]. If the dominant ovarian follicle undergoes atresia, plasma oestrogen levels drop [55]. Additionally, antral follicles must be exposed to sufficiently high levels of FSH for them to escape the onset of atresia [56,57]. In our study, we found that the serum levels of oestradiol and FSH were higher in the NCG group than in the Control group; however, serum levels of progesterone remained unaffected by NCG supplementation. This strongly suggests that NCG likely regulates follicular development by inhibiting follicular atresia.

Increases in follicle sizes are dependent on the replication of granulosa cells, and the formation and expansion of follicular antra [58]. Oestrogen is essential for normal follicular development as it facilitates the differentiation of granulosa cells [59] and improves follicular survival, growth, and antrum formation. Therefore, it is likely that NCG supplementation stimulates the synthesis of oestrogen in ovaries and aids in follicular development.

Since cholesterol is the main precursor molecule required for oestrogen synthesis, we focused on investigating how NCG affected cholesterol metabolism in the ovary. The synthesis of oestrogen in the ovary depends on cholesterol availability and occurs as a collaborative process between thecal cells and granulosa cells. Thecal cells surrounding the follicle convert blood-derived cholesterol into androgens (androstenedione and testosterone) which are passively transported into granulosa cells to be converted into oestrogen (Figure 7). In this process, the amounts of oestrogen synthesised by these ovarian cells are determined by rates of cholesterol uptake and efficiencies of steroidogenic enzymes. Thecal cells obtain cholesterol from LDL-C and HDL-C in the blood; the cholesterol is transported into thecal cells via membrane receptors [60]. In bovine ovaries, the degree of vascularization increases continuously with follicle development [61] to ensure an adequate flow of nutrients, oxygen, and hormonal support from stromal blood vessels [62]. Many endogenous and exogenous factors such as VEGF, angiopoietin, and fibroblast growth factors (FGF) are involved in the regulation of follicular angiogenesis. In our study, we found that NCG supplementation enhanced the xCD31 signal intensity and vascular area percentage in ovaries and upregulated the gene expression of *NOS2* and *VEGFA*, indicating that NCG further promoted angiogenesis in yak ovaries. Furthermore, NCG also increased the gene expression of *SCARB1* and *SCARB2*, although it did not affect serum levels of TC,

LDL-C, HDL-C, or gene expression levels of low-density lipoprotein receptor (*LDLR*). The *SCARB1* and *SCARB2* genes encode scavenger receptor class B type I (SR-BI) and scavenger receptor class B type II (SR-BII), which are considered to be the primary receptors for the uptake of HDL-C molecules [63]. HDLs are the main lipoproteins present in follicular fluid, though smaller amounts of LDL and very low-density lipoproteins (VLDLs) are also present [64,65]; this indicates that HDL is probably absorbed more easily by ovarian cells for steroid synthesis. Our results indicated that NCG supplementation promoted angiogenesis and the uptake of cholesterol in yak ovaries.

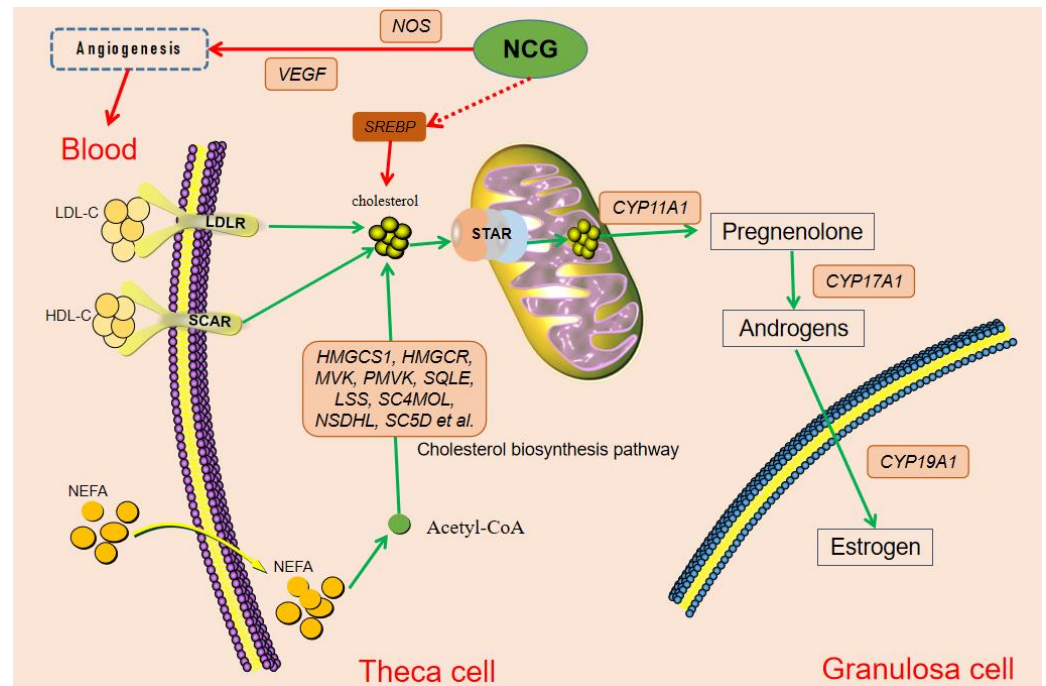


Figure 7. Our proposed model of how N-carbamylglutamate (NCG) regulates cholesterol metabolism, which includes processes related to cholesterol acquisition and steroidogenesis in yak preovulatory ovarian follicles. The red arrows represent processes that NCG affects positively (upregulates) and green arrows represent processes that directly affect cholesterol metabolism.

Similar to most mammalian cells, ovarian cells are able to synthesize cholesterol *de novo* from acetyl-CoA (partly through the beta-oxidation of NEFAs). Cholesterol biosynthesis is a highly regulated process involving more than 20 enzymes, including two enzymes catalysing rate-limiting steps, namely, HMGCR and SQLE [66]. The process is also transcriptionally regulated by the sterol-regulatory element binding protein (SREBP) family of transcription factors [67]. Our analyses of RNA-Seq and RT-PCR data indicated that the gene expression profiles of *SREBP2*, *LSS* (which encodes lanosterol synthase, a key enzyme in the cholesterol biosynthetic pathway [68]), and *SQLE* were upregulated in the NCG group. These results show that NCG promotes the biosynthesis of cholesterol in yak ovaries.

The first step, as well as the rate-limiting step in oestrogen synthesis, is the transport of cholesterol from the outer to the inner mitochondrial membrane [69]. This step is slow and needs to be accelerated by the action of STAR [70], which facilitates cholesterol transfer for the use of cytochrome P450 (CYP) family 17 subfamily A member 1 (CYP11A1) [71]. CYP11A1 cleaves the cholesterol side-chain in the inner mitochondrial membrane to produce pregnenolone [34]. Subsequently, this pregnenolone is converted into androgens (androstenedione and testosterone) by steroid-generating enzymes in theca cells. These androgens are passively transported into granulosa cells to be converted into oestrogen by (CYP) family 19 subfamily A member 1 (CYP19A1) [72]. The schematic representation of oestrogen synthesis is illustrated in Figure 7. Oestrogen is converted into the more

active oestradiol by the protein encoded by the *HSD17B1* gene [73]. Results from our study revealed that NCG supplementation promotes the synthesis of oestrogen in yak ovaries by upregulating the gene expression patterns of all these genes.

In this study, we demonstrated that NCG affects oestrogen synthesis by regulating cholesterol metabolism (Figure 7). Our findings suggest that NCG supplementation could upregulate the expression of NOS2 and VEGFA to promote angiogenesis in yak ovaries, which aid in cholesterol uptake by ovarian cells. Furthermore, NCG also promoted cholesterol biosynthesis and the subsequent oestrogen production. The synthesis of cholesterol and oestrogen are dependent on a series of enzymes which are directly regulated by the mTOR (mechanistic target of rapamycin) signalling pathway. As a precursor of arginine, NCG has been shown to activate the mTOR signalling pathway in numerous studies [74–76]; it is possible that NCG affects cholesterol and oestrogen synthesis through this pathway as well. Overall, we found that NCG supplementation increases the numbers of large follicles (>5 mm in diameter), angiogenesis, and cholesterol metabolism (including cholesterol biosynthesis and its conversion into oestrogen) in yak ovaries.

The limitation of our study was that we only demonstrated the improvement of NCG on the development of yak ovarian follicles with a small number of yak samples. The effects of NCG on the reproduction and productive efficiency (such as conception rate and calving rate) of yak herds need to be further studied. Previous studies reported that supplementation with concentrates or barley straw was helpful for the growth performance [77] and reproduction [5] of grazing yaks. In combination with NCG, these supplements may further improve the reproductive potential of yaks.

5. Conclusions

In summary, our study demonstrated that NCG supplementation promotes ovarian follicular development, which can be confirmed by the increased numbers of large follicles (>5 mm in diameter) formed in yaks fed with NCG. These observations may result from the increased gene expression of angiogenesis factors and enzymes regulating cholesterol metabolism caused by NCG, which has been shown to be a strong promoter of ovarian follicular growth. Therefore, NCG supplementation in concentrate or total mixed ration could be a new reproductive strategy for yaks to improve follicular development and shorten postpartum anoestrus periods.

Supplementary Materials: The following are available online at <https://www.mdpi.com/article/10.3390/agriculture11090825/s1>, Table S1: ingredients and nutrition levels of the basal ration, Table S2: primer sequences used in the real-time PCR, Figure S1: the top 20 enriched GO terms between Control and NCG female yaks, including cellular component, biological process, as well as molecular function, Figure S2. functional classifications of differentially expressed genes (DEGs) in ovarian tissues of Control and NCG group.

Author Contributions: Conceptualization, J.Z., J.D. and B.X. (Bai Xue); formal analysis, J.Z.; funding acquisition, B.X. (Bai Xue); investigation, J.Z. and S.Y.; methodology, J.Z. and J.D.; project administration, B.X. (Bai Xue); software, S.Y.; validation, B.X. (Benchu Xue); writing—original draft, J.Z.; writing—review and editing, J.D., L.W., Q.P. and B.X. (Bai Xue). All authors have read and agreed to the published version of the manuscript.

Funding: The research was supported by the fund for the National Key Research and Development Program of China (2018YFD0502303).

Institutional Review Board Statement: The study was conducted according to the guidelines of the Declaration of Helsinki, and approved by the Animal Care and Ethical Committee of Sichuan Agricultural University (#SCAUAC2020-84).

Informed Consent Statement: Not applicable.

Data Availability Statement: The data supporting the findings of this study can be obtained from the corresponding authors on reasonable request.

Acknowledgments: The authors thank all the members of the Dujiangyan Oujiapo Cattle Farm (Chengdu, China) who provided assistance in handling throughout the experiment. Our deepest gratitude goes to the anonymous reviewers and MDPI team members for their careful work and thoughtful suggestions that have helped improve this paper substantially.

Conflicts of Interest: The authors declare no conflict of interest.

References

1. Guo, X.; Long, R.; Kreuzer, M.; Ding, L.; Shang, Z.; Zhang, Y.; Yang, Y.; Cui, G. Importance of functional ingredients in yak milk-derived food on health of Tibetan nomads living under high-altitude stress: A review. *Crit. Rev. Food Sci. Nutr.* **2014**, *54*, 292–302. [[CrossRef](#)]
2. Qiu, Q.; Zhang, G.; Ma, T.; Qian, W.; Wang, J.; Ye, Z.; Cao, C.; Hu, Q.; Kim, J.; Larkin, D.M. The yak genome and adaptation to life at high altitude. *Nat. Genet.* **2012**, *44*, 946–949. [[CrossRef](#)]
3. Zi, X.-D. Reproduction in female yaks (*Bos grunniens*) and opportunities for improvement. *Theriogenology* **2003**, *59*, 1303–1312. [[CrossRef](#)]
4. Lan, D.; Xiong, X.; Huang, C.; Mipam, T.D.; Li, J. Toward understanding the genetic basis of yak ovary reproduction: A characterization and comparative analyses of estrus ovary transcriptome in yak and cattle. *PLoS ONE* **2016**, *11*, e0152675. [[CrossRef](#)]
5. Long, R.; Zhang, D.; Wang, X.; Hu, Z.; Dong, S. Effect of strategic feed supplementation on productive and reproductive performance in yak cows. *Prev. Vet. Med.* **1999**, *38*, 195–206. [[CrossRef](#)]
6. Fu, M.; Xiong, X.-R.; Lan, D.-L.; Li, J. Molecular characterization and tissue distribution of estrogen receptor genes in domestic yak. *Asian-Australas. J. Anim. Sci.* **2014**, *27*, 1684. [[CrossRef](#)] [[PubMed](#)]
7. Diskin, M.; Kenny, D. Managing the reproductive performance of beef cows. *Theriogenology* **2016**, *86*, 379–387. [[CrossRef](#)] [[PubMed](#)]
8. Peter, A.; Vos, P.; Ambrose, D. Postpartum anestrus in dairy cattle. *Theriogenology* **2009**, *71*, 1333–1342. [[CrossRef](#)] [[PubMed](#)]
9. Kawai, T.; Shimada, M. Pretreatment of ovaries with collagenase before vitrification keeps the ovarian reserve by maintaining cell-cell adhesion integrity in ovarian follicles. *Sci. Rep.* **2020**, *10*, 1–14. [[CrossRef](#)] [[PubMed](#)]
10. Chou, C.-H.; Chen, M.-J. The effect of steroid hormones on ovarian follicle development. *Vitamins* **2018**, *107*, 155–175. [[CrossRef](#)]
11. Tonini, C.; Segatto, M.; Pallottini, V. Impact of Sex and Age on the Mevalonate Pathway in the Brain: A Focus on Effects Induced by Maternal Exposure to Exogenous Compounds. *Metabolites* **2020**, *10*, 304. [[CrossRef](#)]
12. Azhar, S.; Tsai, L.; Medicherla, S.; Chandrasekher, Y.; Giudice, L.; Reaven, E. Human granulosa cells use high density lipoprotein cholesterol for steroidogenesis. *J. Clin. Endocrinol. Metab.* **1998**, *83*, 983–991. [[CrossRef](#)] [[PubMed](#)]
13. Ma, Y.; Zhou, S.; Lin, X.; Zeng, W.; Mi, Y.; Zhang, C. Effect of dietary N-carbamylglutamate on development of ovarian follicles via enhanced angiogenesis in the chicken. *Poult. Sci.* **2020**, *99*, 578–589. [[CrossRef](#)] [[PubMed](#)]
14. Lu, X.; Guo, S.; Cheng, Y.; Kim, J.-H.; Feng, Y. Stimulation of ovarian follicle growth after AMPK inhibition. *Reproduction* **2017**, *153*, 683–694. [[CrossRef](#)] [[PubMed](#)]
15. Yang, M.; Fortune, J. Vascular endothelial growth factor stimulates the primary to secondary follicle transition in bovine follicles in vitro. *Mol. Reprod. Dev.* **2007**, *74*, 1095–1104. [[CrossRef](#)] [[PubMed](#)]
16. Shimizu, T.; Iijima, K.; Ogawa, Y.; Miyazaki, H.; Sasada, H.; Sato, E. Gene injections of vascular endothelial growth factor and growth differentiation factor-9 stimulate ovarian follicular development in immature female rats. *Fertil. Steril.* **2008**, *89*, 1563–1570. [[CrossRef](#)]
17. Shimizu, T.; Iijima, K.; Miyabayashi, K.; Ogawa, Y.; Miyazaki, H.; Sasada, H.; Sato, E. Effect of direct ovarian injection of vascular endothelial growth factor gene fragments on follicular development in immature female rats. *Reproduction* **2007**, *134*, 677–682. [[CrossRef](#)]
18. Quintana, R.; Kopcow, L.; Sueldo, C.; Marconi, G.; Rueda, N.G.; Barañao, R.I. Direct injection of vascular endothelial growth factor into the ovary of mice promotes follicular development. *Fertil. Steril.* **2004**, *82*, 1101–1105. [[CrossRef](#)]
19. Shimizu, T.; Jiang, J.-Y.; Iijima, K.; Miyabayashi, K.; Ogawa, Y.; Sasada, H.; Sato, E. Induction of follicular development by direct single injection of vascular endothelial growth factor gene fragments into the ovary of miniature gilts. *Biol. Reprod.* **2003**, *69*, 1388–1393. [[CrossRef](#)]
20. Abramovich, D.; Irusta, G.; Parborell, F.; Tesone, M. Intrabursal injection of vascular endothelial growth factor trap in eCG-treated prepubertal rats inhibits proliferation and increases apoptosis of follicular cells involving the PI3K/AKT signaling pathway. *Fertil. Steril.* **2010**, *93*, 1369–1377. [[CrossRef](#)]
21. Sargent, K.M.; Lu, N.; Clopton, D.T.; Pohlmeier, W.E.; Brauer, V.M.; Ferrara, N.; Silversides, D.W.; Cupp, A.S. Loss of vascular endothelial growth factor A (VEGFA) isoforms in granulosa cells using pDmrt-1-Cre or Amhr2-Cre reduces fertility by arresting follicular development and by reducing litter size in female mice. *PLoS ONE* **2015**, *10*, e0116332. [[CrossRef](#)]
22. Gao, X.; Zhang, J.; Pan, Z.; Li, Q.; Liu, H. The distribution and expression of vascular endothelial growth factor A (VEGFA) during follicular development and atresia in the pig. *Reprod. Fertil. Dev.* **2020**, *32*, 259–266. [[CrossRef](#)] [[PubMed](#)]
23. Moonmanee, T.; Navanukraw, C.; Uriyapongson, S.; Kraison, A.; Aiumlamai, S.; Guntaprom, S.; Rittirod, T.; Borowicz, P.; Redmer, D. Relationships among vasculature, mitotic activity, and endothelial nitric oxide synthase (eNOS) in bovine antral follicles of the first follicular wave. *Domest. Anim. Endocrinol.* **2013**, *45*, 11–21. [[CrossRef](#)] [[PubMed](#)]

24. Chacher, B.; Wang, D.-M.; Liu, H.-Y.; Liu, J.-X. Degradation of L-arginine and N-carbamoyl glutamate and their effect on rumen fermentation in vitro. *Ital. J. Anim. Sci.* **2012**, *11*, e68. [[CrossRef](#)]
25. Wu, G.; Knabe, D.A.; Kim, S.W. Arginine nutrition in neonatal pigs. *J. Nutr.* **2004**, *134*, 2783S–2790S. [[CrossRef](#)] [[PubMed](#)]
26. Zhu, J.; Zeng, X.; Peng, Q.; Zeng, S.; Zhao, H.; Shen, H.; Qiao, S. Maternal N-carbamylglutamate supplementation during early pregnancy enhances embryonic survival and development through modulation of the endometrial proteome in gilts. *J. Nutr.* **2015**, *145*, 2212–2220. [[CrossRef](#)]
27. Zhang, H.; Sun, H.; Peng, A.; Guo, S.; Wang, M.; Loor, J.J.; Wang, H. N-carbamylglutamate and l-arginine promote intestinal function in suckling lambs with intrauterine growth restriction by regulating antioxidant capacity via a nitric oxide-dependent pathway. *Food Funct.* **2019**, *10*, 6374–6384. [[CrossRef](#)] [[PubMed](#)]
28. Liu, X.; Wu, X.; Yin, Y.; Liu, Y.; Geng, M.; Yang, H.; Blachier, F.; Wu, G.J.A.a. Effects of dietary L-arginine or N-carbamylglutamate supplementation during late gestation of sows on the miR-15b/16, miR-221/222, VEGFA and eNOS expression in umbilical vein. *Amino Acids* **2012**, *42*, 2111–2119. [[CrossRef](#)]
29. Zhang, H.; Peng, A.; Guo, S.; Wang, M.; Loor, J.J.; Wang, H. Dietary N-carbamylglutamate and l-arginine supplementation improves intestinal energy status in intrauterine-growth-retarded suckling lambs. *Food Funct.* **2019**, *10*, 1903–1914. [[CrossRef](#)]
30. Wang, H.; Lin, C.; Yao, J.; Shi, H.; Zhang, C.; Wei, Q.; Lu, Y.; Chen, Z.; Xing, G.; Cao, X. Deletion of OSBPL2 in auditory cells increases cholesterol biosynthesis and drives reactive oxygen species production by inhibiting AMPK activity. *Cell Death Dis.* **2019**, *10*, 1–13. [[CrossRef](#)]
31. Zhang, H.; Zhao, F.; Nie, H.; Ma, T.; Wang, Z.; Wang, F.; Loor, J.J. Dietary N-carbamylglutamate and rumen-protected l-arginine supplementation during intrauterine growth restriction in undernourished ewes improve fetal thymus development and immune function. *Reprod. Fertil. Dev.* **2018**, *30*, 1522–1531. [[CrossRef](#)]
32. Chacher, B.; Zhu, W.; Ye, J.; Wang, D.; Liu, J. Effect of dietary N-carbamoylglutamate on milk production and nitrogen utilization in high-yielding dairy cows. *J. Dairy Sci.* **2014**, *97*, 2338–2345. [[CrossRef](#)] [[PubMed](#)]
33. Armstrong, D.G.; McEvoy, T.; Baxter, G.; Robinson, J.; Hogg, C.; Woad, K.; Webb, R.; Sinclair, K. Effect of dietary energy and protein on bovine follicular dynamics and embryo production in vitro: Associations with the ovarian insulin-like growth factor system. *Biol. Reprod.* **2001**, *64*, 1624–1632. [[CrossRef](#)] [[PubMed](#)]
34. Walsh, S.W.; Mehta, J.P.; McGettigan, P.A.; Browne, J.A.; Forde, N.; Alibrahim, R.; Mulligan, F.; Loftus, B.; Crowe, M.A.; Matthews, D. Effect of the metabolic environment at key stages of follicle development in cattle: Focus on steroid biosynthesis. *Physiol. Genom.* **2012**, *44*, 504–517. [[CrossRef](#)] [[PubMed](#)]
35. Ying, S.; Wang, Z.; Wang, C.; Nie, H.; He, D.; Jia, R.; Wu, Y.; Wan, Y.; Zhou, Z.; Yan, Y. Effect of different levels of short-term feed intake on folliculogenesis and follicular fluid and plasma concentrations of lactate dehydrogenase, glucose, and hormones in Hu sheep during the luteal phase. *Reproduction* **2011**, *142*, 699. [[CrossRef](#)]
36. Miura, R. Physiological characteristics and effects on fertility of the first follicular wave dominant follicle in cattle. *J. Reprod. Dev.* **2019**, *65*, 289. [[CrossRef](#)] [[PubMed](#)]
37. Cui, Y.; Yu, S. An anatomical study of the internal genital organs of the yak at different ages. *Vet. J.* **1999**, *157*, 192–196. [[CrossRef](#)]
38. Gohir, W.; Kennedy, K.M.; Wallace, J.G.; Saoi, M.; Bellissimo, C.J.; Britz-McKibbin, P.; Petrik, J.J.; Surette, M.G.; Sloboda, D.M. High-fat diet intake modulates maternal intestinal adaptations to pregnancy and results in placental hypoxia, as well as altered fetal gut barrier proteins and immune markers. *J. Physiol.* **2019**, *597*, 3029–3051. [[CrossRef](#)]
39. Wong, Y.L.; LeBon, L.; Basso, A.M.; Kohlhaas, K.L.; Nikkel, A.L.; Robb, H.M.; Donnelly-Roberts, D.L.; Prakash, J.; Swensen, A.M.; Rubinstein, N.D. eIF2B activator prevents neurological defects caused by a chronic integrated stress response. *Elife* **2019**, *8*, e42940. [[CrossRef](#)]
40. Chen, S.; Zhou, Y.; Chen, Y.; Gu, J. fastp: An ultra-fast all-in-one FASTQ preprocessor. *Bioinformatics* **2018**, *34*, i884–i890. [[CrossRef](#)]
41. Anders, S.; Pyl, P.T.; Huber, W. HTSeq—A Python framework to work with high-throughput sequencing data. *Bioinformatics* **2015**, *31*, 166–169. [[CrossRef](#)]
42. Kim, D.; Langmead, B.; Salzberg, S.L. HISAT: A fast spliced aligner with low memory requirements. *Nat. Methods* **2015**, *12*, 357–360. [[CrossRef](#)]
43. Pertea, M.; Pertea, G.M.; Antonescu, C.M.; Chang, T.-C.; Mendell, J.T.; Salzberg, S.L. StringTie enables improved reconstruction of a transcriptome from RNA-seq reads. *Nat. Biotechnol.* **2015**, *33*, 290–295. [[CrossRef](#)] [[PubMed](#)]
44. Pertea, M.; Kim, D.; Pertea, G.M.; Leek, J.T.; Salzberg, S.L. Transcript-level expression analysis of RNA-seq experiments with HISAT, StringTie and Ballgown. *Nat. Protoc.* **2016**, *11*, 1650–1667. [[CrossRef](#)] [[PubMed](#)]
45. Love, M.I.; Huber, W.; Anders, S. Moderated estimation of fold change and dispersion for RNA-seq data with DESeq2. *Genome Biol.* **2014**, *15*, 1–21. [[CrossRef](#)] [[PubMed](#)]
46. Livak, K.J.; Schmittgen, T.D. Analysis of relative gene expression data using real-time quantitative PCR and the $2^{-\Delta\Delta CT}$ method. *Methods* **2001**, *25*, 402–408. [[CrossRef](#)] [[PubMed](#)]
47. Sirois, J.; Fortune, J. Ovarian follicular dynamics during the estrous cycle in heifers monitored by real-time ultrasonograph. *Biol. Reprod.* **1988**, *39*, 308–317. [[CrossRef](#)]
48. Ginther, O.; Beg, M.; Bergfelt, D.; Donadeu, F.; Kot, K. Follicle selection in monovular species. *Biol. Reprod.* **2001**, *65*, 638–647. [[CrossRef](#)]
49. Adams, G.; Jaiswal, R.; Singh, J.; Malhi, P. Progress in understanding ovarian follicular dynamics in cattle. *Theriogenology* **2008**, *69*, 72–80. [[CrossRef](#)]

50. Labrecque, R.; Fournier, E.; Sirard, M.A. Transcriptome analysis of bovine oocytes from distinct follicle sizes: Insights from correlation network analysis. *Mol. Reprod. Dev.* **2016**, *83*, 558–569. [[CrossRef](#)]
51. Lequarre, A.-S.; Vigneron, C.; Ribaucour, F.; Holm, P.; Donnay, I.; Dalbies-Tran, R.; Callesen, H.; Mermillod, P. Influence of antral follicle size on oocyte characteristics and embryo development in the bovine. *Theriogenology* **2005**, *63*, 841–859. [[CrossRef](#)] [[PubMed](#)]
52. Blondin, P.; Sirard, M.A. Oocyte and follicular morphology as determining characteristics for developmental competence in bovine oocytes. *Mol. Reprod. Dev.* **1995**, *41*, 54–62. [[CrossRef](#)] [[PubMed](#)]
53. Jolly, P.; Tisdall, D.; Heath, D.; Lun, S.; McNatty, K. Apoptosis in bovine granulosa cells in relation to steroid synthesis, cyclic adenosine 3', 5'-monophosphate response to follicle-stimulating hormone and luteinizing hormone, and follicular atresia. *Biol. Reprod.* **1994**, *51*, 934–944. [[CrossRef](#)] [[PubMed](#)]
54. Grimes, R.; Matton, P.; Ireland, J. A comparison of histological and non-histological indices of atresia and follicular function. *Biol. Reprod.* **1987**, *37*, 82–88. [[CrossRef](#)] [[PubMed](#)]
55. Sasagawa, S.; Shimizu, Y.; Nagaoka, T.; Tokado, H.; Imada, K.; Mizuguchi, K. Dienogest, a selective progestin, reduces plasma estradiol level through induction of apoptosis of granulosa cells in the ovarian dominant follicle without follicle-stimulating hormone suppression in monkeys. *J. Endocrinol. Investig.* **2008**, *31*, 636–641. [[CrossRef](#)]
56. Chun, S.; Eisenhauer, K.M.; Minami, S.; Billig, H.; Perlas, E.; Hsueh, A. Hormonal regulation of apoptosis in early antral follicles: Follicle-stimulating hormone as a major survival factor. *Endocrinology* **1996**, *137*, 1447–1456. [[CrossRef](#)]
57. Kaipia, A.; Hsueh, A.J. Regulation of ovarian follicle atresia. *Annu. Rev. Physiol.* **1997**, *59*, 349–363. [[CrossRef](#)]
58. Goldenberg, R.; Vaitukaitis, J.; ROSS, G.T. Estrogen and follicle stimulating hormone interactions on follicle growth in rats. *Endocrinology* **1972**, *90*, 1492–1498. [[CrossRef](#)] [[PubMed](#)]
59. Drummond, A.E.; Findlay, J.K. The role of estrogen in folliculogenesis. *Mol. Cell. Endocrinol.* **1999**, *151*, 57–64. [[CrossRef](#)]
60. Chang, X.-L.; Liu, L.; Wang, N.; Chen, Z.-J.; Zhang, C. The function of high-density lipoprotein and low-density lipoprotein in the maintenance of mouse ovarian steroid balance. *Biol. Reprod.* **2017**, *97*, 862–872. [[CrossRef](#)]
61. Robinson, R.; Hammond, A.; Nicklin, L.; Schams, D.; Mann, G.; Hunter, M. Endocrine and cellular characteristics of corpora lutea from cows with a delayed post-ovulatory progesterone rise. *Domest. Anim. Endocrinol.* **2006**, *31*, 154–172. [[CrossRef](#)]
62. Robinson, R.; Woad, K.; Hammond, A.; Laird, M.; Hunter, M.; Mann, G. Angiogenesis and vascular function in the ovary. *Reproduction* **2009**, *138*, 869–881. [[CrossRef](#)] [[PubMed](#)]
63. Zeng, T.-T.; Tang, D.-J.; Ye, Y.-X.; Su, J.; Jiang, H. Influence of SCARB1 gene SNPs on serum lipid levels and susceptibility to coronary heart disease and cerebral infarction in a Chinese population. *Gene* **2017**, *626*, 319–325. [[CrossRef](#)]
64. Gautier, T.; Becker, S.; Drouineaud, V.; Ménétrier, F.; Sagot, P.; Nofer, J.-R.; von Otte, S.; Lagrost, L.; Masson, D.; Tietge, U.J. Human luteinized granulosa cells secrete apoB100-containing lipoproteins. *J. Lipid Res.* **2010**, *51*, 2245–2252. [[CrossRef](#)] [[PubMed](#)]
65. Quiroz, A.; Molina, P.; Santander, N.; Gallardo, D.; Rigotti, A.; Busso, D. Ovarian cholesterol efflux: ATP-binding cassette transporters and follicular fluid HDL regulate cholesterol content in mouse oocytes. *Biol. Reprod.* **2020**, *102*, 348–361. [[CrossRef](#)] [[PubMed](#)]
66. Tan, J.M.; Cook, E.C.; van den Berg, M.; Scheij, S.; Zelcer, N.; Loregger, A. Differential use of E2 ubiquitin conjugating enzymes for regulated degradation of the rate-limiting enzymes HMGCR and SQLE in cholesterol biosynthesis. *Atherosclerosis* **2019**, *281*, 137–142. [[CrossRef](#)] [[PubMed](#)]
67. Brown, M.S.; Goldstein, J.L. The SREBP pathway: Regulation of cholesterol metabolism by proteolysis of a membrane-bound transcription factor. *Cell Adhes. Commun.* **1997**, *89*, 331–340. [[CrossRef](#)]
68. Romano, M.-T.; Tafazzoli, A.; Mattern, M.; Sivalingam, S.; Wolf, S.; Rupp, A.; Thiele, H.; Altmüller, J.; Nürnberg, P.; Ellwanger, J. Bi-allelic mutations in LSS, encoding lanosterol synthase, cause autosomal-recessive hypotrichosis simplex. *Am. J. Hum. Genet.* **2018**, *103*, 777–785. [[CrossRef](#)]
69. Black, S.M.; Harikrishna, J.A.; Szklarz, G.D.; Miller, W.L. The mitochondrial environment is required for activity of the cholesterol side-chain cleavage enzyme, cytochrome P450_{sc}. *Proc. Natl. Acad. Sci. USA* **1994**, *91*, 7247–7251. [[CrossRef](#)]
70. Clark, B.J.; Wells, J.; King, S.R.; Stocco, D.M. The purification, cloning, and expression of a novel luteinizing hormone-induced mitochondrial protein in MA-10 mouse Leydig tumor cells. Characterization of the steroidogenic acute regulatory protein (StAR). *J. Biol. Chem.* **1994**, *269*, 28314–28322. [[CrossRef](#)]
71. Kallen, C.B.; Billheimer, J.T.; Summers, S.A.; Stayrook, S.E.; Lewis, M.; Strauss, J.F. Steroidogenic acute regulatory protein (StAR) is a sterol transfer protein. *J. Biol. Chem.* **1998**, *273*, 26285–26288. [[CrossRef](#)]
72. Parween, S.; DiNardo, G.; Baj, F.; Zhang, C.; Gilardi, G.; Pandey, A.V. Differential effects of variations in human P450 oxidoreductase on the aromatase activity of CYP19A1 polymorphisms R264C and R264H. *J. Steroid Biochem. Mol. Biol.* **2020**, *196*, 105507. [[CrossRef](#)] [[PubMed](#)]
73. Yuan, X.; Zhou, X.; Qiao, X.; Wu, Q.; Yao, Z.; Jiang, Y.; Zhang, H.; Zhang, Z.; Wang, X.; Li, J. FoxA2 and p53 regulate the transcription of HSD17B1 in ovarian granulosa cells of pigs. *Reprod. Domest. Anim.* **2021**, *56*, 74–82. [[CrossRef](#)]
74. Zhang, H.; Peng, A.; Yu, Y.; Guo, S.; Wang, M.; Coleman, D.N.; Loo, J.J.; Wang, H. N-Carbamylglutamate and l-arginine promote intestinal absorption of amino acids by regulating the mTOR signaling pathway and amino acid and peptide transporters in suckling lambs with intrauterine growth restriction. *J. Nutr.* **2019**, *149*, 923–932. [[CrossRef](#)] [[PubMed](#)]
75. Huang, F.; Sun, Y.; Gao, H.; Wu, H.; Wang, Z. Carbon disulfide induces embryo loss by perturbing the expression of the mTOR signalling pathway in uterine tissue in mice. *Chem.-Biol. Interact.* **2019**, *300*, 8–17. [[CrossRef](#)] [[PubMed](#)]

-
76. Zeng, X.; Huang, Z.; Mao, X.; Wang, J.; Wu, G.; Qiao, S. N-carbamylglutamate enhances pregnancy outcome in rats through activation of the PI3K/PKB/mTOR signaling pathway. *PLoS ONE* **2012**, *7*, e41192. [[CrossRef](#)] [[PubMed](#)]
 77. Ding, L.; Chen, J.; Long, R.; Gibb, M.J.; Wang, L.; Sang, C.; Mi, J.; Zhou, J.; Liu, P.; Shang, Z.; et al. Blood hormonal and metabolite levels in grazing yak steers undergoing compensatory growth. *J. Anim. Feed Sci.* **2015**, *209*, 30–39. [[CrossRef](#)]